

# Calculation of the Free Energy Profile of H<sub>2</sub>O, O<sub>2</sub>, CO, CO<sub>2</sub>, NO, and CHCl<sub>3</sub> in a Lipid Bilayer with a Cavity Insertion Variant of the Widom Method

Pál Jedlovsky<sup>†</sup> and Mihaly Mezei\*

Contribution from the Department of Physiology and Biophysics, Mount Sinai School of Medicine of the New York University, New York, New York 10029

Received January 14, 2000. Revised Manuscript Received March 28, 2000

**Abstract:** The excess free energy profile of H<sub>2</sub>O, O<sub>2</sub>, CO, CO<sub>2</sub>, NO, and CHCl<sub>3</sub> has been computed across a fully hydrated dimyristoylphosphatidylcholine (DMPC) bilayer by a cavity insertion variant of the Widom test particle method. This Cavity Insertion Widom (CIW) method modifies the original Widom procedure in such a way that, analogously to the cavity biased particle insertions used in grand canonical and Gibbs ensemble Monte Carlo simulations, it inserts the test particle into cavities of suitable radius only. Results on aqueous systems show that this modification can make the Widom method considerably faster and also more accurate. The free energy profiles obtained are in accordance with the physiological properties of the investigated molecules. It is found that the interior of the membrane constitutes a free energy barrier of about 13 kcal/mol for H<sub>2</sub>O, and a free energy well of 3–4 kcal/mol for O<sub>2</sub>, CO, and NO. In contrast to these four free energy profiles, which change monotonically between the two phases of the membrane, the free energy profile of CO<sub>2</sub> has about 4 kcal/mol deep wells in the two interfacial regions. While, due to its larger size, the results for CHCl<sub>3</sub> are considerably less accurate than for the other five solutes it could still be concluded that its excess free energy is a few kilocalories per mole lower in the interior of the membrane than in the aqueous phase, and the headgroup regions constitute large free energy barriers.

## I. Introduction

The transport of small molecules across the membrane of living cells is of key importance in almost every biochemical processes. While various regulatory mechanisms are responsible for most of these biologically important transport processes (e.g., the crossmembrane transport of any kind of ions involves special membrane-bound protein molecules<sup>1</sup>), several small, uncharged molecules of vital biological importance, e.g., water, O<sub>2</sub>, CO, CO<sub>2</sub>, NO, N<sub>2</sub>O, CHCl<sub>3</sub>, formamide, or urea, can permeate the cell membrane without the aid of any transmembrane proteins.<sup>2–4</sup> The transport of these molecules across cell membranes can be of vital importance in several physiological processes. For instance, the entire respiratory mechanism is based on the exchange of CO<sub>2</sub> and O<sub>2</sub> molecules between the red blood cells and the outside environment. The NO molecule is a key element of the blood pressure regulation mechanism,<sup>4</sup> in part due to its ability to cross promptly the cell membrane. The crossmembrane transport properties of N<sub>2</sub>O and CHCl<sub>3</sub> make them widely used anaesthetics.

Although computer simulation methods can, in principle, provide great help in the understanding of these transport processes at a molecular level, very little has been done in this direction so far. The main reason of the lack of such studies is

the enormous computing capacity needed to simulate the transmembrane penetration of a single molecule. For instance, the flux of the water molecules across a cell membrane is in the order of 10<sup>-5</sup> molecules/Å<sup>2</sup> ns,<sup>5</sup> several orders of magnitude smaller than what can be observed in the computationally accessible scale of the presently available molecular dynamics (MD) simulations.

From a thermodynamic point of view, transport processes are governed by the free energy gradient of the moving molecule. Thus, instead of simulating the transmembrane penetration of small, uncharged molecules directly, the calculation of their free energy profiles across the membrane can also shed some light on the physicochemical background of their crossmembrane transport. However, calculation of solvation free energies is a computationally far more demanding task than the generation of an equilibrium ensemble by computer simulations.<sup>6,7</sup> This difficulty is exacerbated for inhomogeneous systems, such as lipid bilayers that combine aqueous, hydrophobic, and mixed hydrophobic–zwitterionic regions, since it lacks the degeneracy that helps to reduce significantly the statistical errors for homogeneous systems. Furthermore, the slow pace of conformational changes of the lipid molecules gives rise to large local differences during the typical simulation time scale, adding another dimension to the system's inhomogeneity. As a result, free energy profiles across the bilayer calculated with methods well tested in aqueous environment can display strong dependence on the region of the bilayer used for the calculation<sup>8</sup> and can thus be unreliable.

\* Address correspondence to this author.

<sup>†</sup> On leave from the Chemical Research Center of the Hungarian Academy of Sciences, Budapest, Hungary.

(1) Hille, B. *Ionic Channels of Excitable Membranes*; Sinauer Associates: Sunderland, 1992.

(2) Guyton, A. C.; Hall, J. E. *Textbook of Medical Physiology*; W. B. Saunders: Philadelphia, 1996.

(3) Finkelstein, A. J. *Gen. Physiol.* **1976**, *68*, 127.

(4) Garthwaite, J.; Boulton, C. L. *Annu. Rev. Physiol.* **1995**, *57*, 683.

(5) Marrink, S. J.; Berendsen, H. J. C. *J. Phys. Chem.* **1994**, *98*, 4155.

(6) Mezei, M.; Beveridge, D. L. *Ann. Acad. Sci. N.Y.* **1986**, *482*, 1.

(7) Straatsma T. P.; McCammon, J. A. *Annu. Rev. Phys. Chem.* **1992**, *43*, 407.

Due to these difficulties, besides several computational studies of free energy profiles of apolar solutes limited to the hydrocarbon phase of the membrane,<sup>9,10</sup> such free energy profile calculation across a fully hydrated lipid bilayer has, to our knowledge, been reported only once, in the pioneering work of Marrink and Berendsen.<sup>5</sup> They calculated the free energy profile of water across a bilayer of dipalmitoylphosphatidylcholine (DPPC) molecules. However, this calculation was rather complicated, since different methods were used in the different regions of the membrane. Namely, the excess free energy of water was estimated from its local density, from the mean force acting on constrained molecules, and by the Widom test particle insertion method<sup>11</sup> in the aqueous, interfacial, and apolar region of the bilayer, respectively. Besides its computational cost, this approach also has the serious limitation that it takes advantage of the fact that the bilayer is in an aqueous environment, and therefore it cannot be applied for any molecule other than water.

A relatively simple and fast way of determining the free energy profile of various molecules across a lipid membrane can be the cavity insertion version of the well-known Widom test particle insertion method.<sup>11</sup> Variants of this method have already been successfully applied for several simpler systems, e.g., the chemical potential of Lennard-Jones liquids,<sup>12</sup> the free energy profile of fluorinated methanes across water–hexane interface and a hydrated bilayer of glycerol-1-monooleate,<sup>13</sup> and the solubility of water, methane and ethanol in various polymers and liquids<sup>14</sup> have been calculated in this way. In the Cavity Insertion Widom (CIW) calculation the test particle is only inserted into cavities of suitable radius. This modification can speed up the convergence of the calculation by several orders of magnitude. The CIW method has the additional advantage that once representative configurations of the pure lipid membrane are generated, the calculation of the free energy profile itself is rather fast, and thus it can rapidly and easily be performed for a set of different molecules. In this paper, we validate the CIW method by determining the precision obtainable with it by comparisons of the excess free energy of six different molecules, i.e., H<sub>2</sub>O, O<sub>2</sub>, CO, CO<sub>2</sub>, NO, and CHCl<sub>3</sub>, in water, as obtained with the CIW and the original Widom method. Further validation of the particle insertion technique for these systems is also obtained by comparing these results with the excess free energy obtained in completely different ways. For this purpose we used the thermodynamic integration method<sup>6</sup> over a polynomial path<sup>15</sup> that mutates an ideal gas particle into the solute for all six molecules, and also grand canonical ensemble Monte Carlo simulation for water. Finally, the applicability of the CIW method for small neutral molecules in a lipid membrane is demonstrated by calculating the free energy profile of the above six molecules across a dimyristoylphosphatidylcholine (DMPC) bilayer.

The paper is organized as follows. In section II the CIW method is described, in section III details of the calculations performed are given, in section IV the results obtained are discussed, and finally in section V some conclusions are drawn.

## II. The Cavity Insertion Widom Method

The original Widom insertion method<sup>11</sup> obtains the excess chemical potential  $\mu'$  of a molecule by inserting it at random positions and in random orientations into Boltzmann-sampled configuration of a system of  $N$  molecules.  $\mu'$  is calculated as

$$\mu' = -k_B T \ln \langle \exp(-E_{N+1}/k_B T) \rangle \quad (1)$$

where  $k_B$  is the Boltzmann constant,  $T$  is the absolute temperature,  $E_{N+1}$  is the energy of the interaction between the randomly inserted molecule and the rest of the system, and  $\langle \dots \rangle$  denotes ensemble averaging over all positions and orientations of the inserted molecule. The excess Helmholtz free energy of the molecule can then simply be obtained from the relation

$$A' = \mu' - pV/N + k_B T \quad (2)$$

where  $p$  and  $V$  are the pressure and volume of the system, respectively. It has been remarked by Sharp<sup>16</sup> that this is equivalent to a simulation using the  $(N + 1)$ -th molecule as an ideal gas and employing the popular perturbation method formula<sup>17</sup> to obtain the free energy of mutating it into a real molecule.

However, with increasing density (or with increasing size of the  $(N + 1)$ -th molecule) random insertions will produce progressively less frequently energies that are sufficiently low to give significant contributions to the average in eq 1 making the calculated average unreliable. This has been demonstrated by Guillot and Guissani<sup>18</sup> in their studies of hydrophobic hydration. This is similar to the difficulty that the grand-canonical ensemble (GCE) simulations face in the particle creation step.<sup>19</sup> It was shown, however, that by using preexisting cavities for insertions<sup>20,21</sup> GCE simulations can be performed in significantly denser systems than was possible before. This idea can also be extended to the Widom method and provides a more efficient variant.

While the original Widom method calculates the energies of randomly inserted molecules, the cavity insertion variant used in this paper first selects cavities of minimum radius  $R_{\text{cav}}$  and inserts test particles only there. In this case, the right-hand side of eq 1 gives the free energy of mutating a cavity into our molecule. Thus, to obtain the excess chemical potential, eq 1 has to include the free energy of forming that cavity:

$$\mu' = -k_B T \ln \langle \exp(-E_{N+1}/k_B T) \rangle - k_B T \ln \langle P_{\text{cav}} \rangle \quad (3)$$

where  $P_{\text{cav}}$  is the probability of finding a cavity of radius at least  $R_{\text{cav}}$ . Equation 3 is the formal equivalent of the Excluded Volume Map Sampling technique of Deitrick et al.<sup>12</sup> It differs from the method of Pohorille and Wilson<sup>13</sup> in that it does not consider the distribution of cavities of various sizes and thereby simplifies the calculation (albeit possibly at the expense of some loss of precision). Such calculation can be realized by setting up a grid in the simulation cell, compiling a list of gridpoints that are centers of a cavity, and inserting new molecules only at those points.  $P_{\text{cav}}$  can immediately be obtained as the ratio of cavities found to the number of grid points. As described in ref 21, the cavity gridpoints can be found efficiently by a scan of the  $N$  molecules in the system, by marking all gridpoints that are covered by them. At the end of the scan, all gridpoints left unmarked are centers of cavities. Since the system moves between insertion attempts, the grid has to be scanned each time before insertions are performed. This also allows the random shifting of the grid without computational penalty, eliminating a possible source of error stemming from the finiteness of the grid.

It is important to emphasize that the CIW method is still limited to solutes whose size is commensurate with the largest cavities found in the system. Thus, for each new solute it is advisable to test it in a pure

(8) Jedlovsky, P. Unpublished results.

(9) Bassolino-Klimas, D.; Alper, H. E.; Stouch, T. R. *J. Am. Chem. Soc.* **1995**, *117*, 4118.

(10) Stouch, T. R.; Bassolino, D. In *Biological Membranes*; Merz, K. M., Roux, B., Eds.; Birkhäuser: Boston, 1996; pp 255–280.

(11) Widom, B. *J. Chem. Phys.* **1963**, *39*, 2808.

(12) Deitrick, G. L.; Scriven, L. E.; Davis, H. T. *J. Chem. Phys.* **1989**, *90*, 2370.

(13) Pohorille, A.; Wilson, M. A. *J. Chem. Phys.* **1996**, *104*, 3760.

(14) Tamai, Y.; Tanaka, H.; Nakanishi, K. *Fluid Phase Equilibria* **1995**, *104*, 363.

(15) Mezei, M. *J. Comput. Chem.* **1992**, *13*, 651.

(16) Sharp, K. Private communication.

(17) Zwanzig, R. W. *J. Chem. Phys.* **1954**, *22*, 1420.

(18) Guillot, B.; Guissani, Y. *J. Chem. Phys.* **1993**, *99*, 8075.

(19) Adams, D. J. *Mol. Phys.* **1975**, *29*, 311.

(20) Mezei, M. *Mol. Phys.* **1980**, *40*, 901.

(21) Mezei, M. *Mol. Phys.* **1987**, *61*, 565. Erratum: **1989**, *67*, 1207.

**Table 1.** Interaction Parameters of the Studied Molecules

molecule	atom	$\sigma/\text{\AA}$	$\epsilon/\text{kcal mol}^{-1}$	$q/e$
H <sub>2</sub> O	H			+0.417
	O	3.151	0.152	-0.834
O <sub>2</sub>	O	3.029	0.120	0
	C	3.742	0.110	+0.021
CO	O	3.029	0.120	-0.021
	C	3.262	0.123	+0.663
CO <sub>2</sub>	O	3.014	0.194	0.3315
	N	3.250	0.170	+0.028
NO	O	3.120	0.159	-0.028
	CH	3.800	0.080	+0.420
CHCl <sub>3</sub>	CH	3.800	0.080	+0.420
	Cl	3.470	0.400	-0.140

solvent system where the excess Helmholtz free energy can be calculated by different methods as well.

The CIW method is conceptually related to one-step free energy methods as implemented by Mark et al.<sup>22</sup>

### III. Calculation Details

**A. Simulations in Aqueous Environment.** To determine the precision obtainable with the Cavity Insertion Widom method, we have determined the excess free energy of six different molecules, H<sub>2</sub>O, O<sub>2</sub>, CO, CO<sub>2</sub>, NO, and CHCl<sub>3</sub>, in pure water with both the original Widom and the CIW method. In all of these calculations the excess particle was inserted into equilibrium configurations of 107 water molecules, obtained from ( $N, V, T$ ) ensemble Monte Carlo (MC) simulations at 310 K. The cubic simulation box was used with the edge length of 14.74 Å, to ensure the experimental density. The pressure of this system was found to be -676 bar.

The interaction of two molecules was described as a sum of charge-charge and Lennard-Jones interactions between their atoms, using the Lorentz-Berthelot mixing rule in the latter case. The water molecules were described by the TIP3P model,<sup>23</sup> the parameters of the CO and O<sub>2</sub> molecules were taken from the CHARMM library,<sup>24</sup> and those of the CO<sub>2</sub>,<sup>25</sup> NO,<sup>26</sup> and CHCl<sub>3</sub><sup>27</sup> molecules were taken from the literature. The interaction parameters of the six molecules studied are summarized in Table 1. The molecules were rigid in all cases: the bond lengths of H<sub>2</sub>O, O<sub>2</sub>, CO, CO<sub>2</sub>, NO, and CHCl<sub>3</sub> were 0.957, 1.208, 1.128, 1.230, 1.150, and 1.758 Å, respectively. In the case of the CHCl<sub>3</sub> molecule the CH group was treated as a united atom. The H-O-H angle of water, the O-C-O angle of CO<sub>2</sub>, and the Cl-C-Cl angle of the CHCl<sub>3</sub> molecule were set to 104.5°, 180.0°, and 111.3°, respectively.

In each Monte Carlo step a water molecule was randomly displaced by no more than 0.2 Å and rotated around a randomly selected space-fixed axis by a maximum angle of 17.5°. The systems were equilibrated by  $2 \times 10^6$  MC moves. Subsequently,  $2 \times 10^7$  new configurations were generated, among which 40 000 ones, separated by 500 MC steps each, were used in the excess free energy calculation. In the original Widom calculations the test particle was inserted into 3375 different points in 10 different, randomly chosen orientations in each of the sample configurations. In the case of the CIW calculations 216 000 points were checked in every sample configurations, and the test particle was only inserted, again in 10 different orientations, at points that were located in a cavity of radius at least  $R_{\text{cav}}$ . All the CIW calculations were performed with two different  $R_{\text{cav}}$  values, 2.6 and 2.8 Å. These

(22) Mark, A. E.; Schäfer, H.; Liu, H.; van Gunsteren, W. In *Computational Molecular Dynamics, Challenges, Methods, Ideas*; Deuffhard, J., Hermans, J., Leimkuhler, B., Mark, A., Reich, S. R. D., Skeel, R. D., Eds.; Springer: New York, 1999; pp 149-162.

(23) Jorgensen, W. L.; Chandrashekar, J.; Madura, J. D.; Impey, R.; Klein, M. L. *J. Chem. Phys.* **1983**, *79*, 926.

(24) Schlenker, M.; Brickmann, J.; MacKerell, A. D., Jr.; Karplus, M. In *Biological Membranes*; Merz, K. M., Roux, B., Eds.; Birkhäuser: Boston, 1996; pp 31-82.

(25) Somasundaram, T., In: het Panhuis, M.; Lynden-Bell, R. M.; Patterson, C. H. *J. Chem. Phys.* **1999**, *111*, 2190.

(26) Li, H.; Elber, R.; Straub, J. E. *J. Biol. Chem.* **1983**, *268*, 17908.

(27) Jorgensen, W. L.; Briggs, J. M.; Contreras, M. L. *J. Phys. Chem.* **1990**, *94*, 1683.

calculations were 15-20% and about 4 times faster respectively than when the original Widom method was used.

To test the convergence of the averages of eqs 1 and 3 in the simulations, we have also determined the excess free energy of the above six molecules in water using the thermodynamic integration (TI) methodology<sup>6</sup> over a polynomial path.<sup>15</sup> Here we parametrized the solute-solvent contribution to the system's energy as

$$E(\lambda) = \lambda^{k_{12}} E^{12} + \lambda^{k_6} E^6 + \lambda^{k_1} E^1 \quad (4)$$

where  $\lambda$  is the coupling parameter between the free and the hydrated solute molecule, and  $E^{12}$ ,  $E^6$ , and  $E^1$  are the energy contributions containing the  $1/r$ ,<sup>12</sup>  $1/r^6$ , and  $1/r$  terms, respectively. The excess free energy of the solute molecule can then be obtained as

$$A' = \int_0^1 k_{12} \lambda^{k_{12}-1} \langle E^{12} \rangle_\lambda + k_6 \lambda^{k_6-1} \langle E^6 \rangle_\lambda + k_1 \lambda^{k_1-1} \langle E^1 \rangle_\lambda d\lambda \quad (5)$$

Here  $\langle \dots \rangle_\lambda$  indicates that the ensemble averages were computed using  $E(\lambda)$  instead of the solute-solvent internal energy contribution in the Boltzmann factor. The exponents  $k_{12}$ ,  $k_6$ , and  $k_1$  were chosen to be 4, 3, and 3, respectively, for water and 4, 3, and 2 for the other five solutes, to make the integrand as close to linear as possible. The integral of eq 5 was evaluated using a 5-point Gaussian quadrature, i.e., the integrand was determined at the  $\lambda$  values of 0.04691, 0.230765, 0.5, 0.769235, and 0.95309 by performing a MC simulation at each point. These simulations were performed in the same way as in the case of the CIW calculations. The excess Helmholtz free energy results were well converged after  $10^7$  MC steps per quadrature points. The excess free energy was obtained about 3 and 10-12 times faster in this way than by the CIW method with  $R_{\text{cav}} = 2.8$  and 2.6 Å, respectively, and about 13-15 times faster than by the original Widom method, which demonstrates the remarkable computational efficiency of the thermodynamic integration over a polynomial path for homogeneous systems.

In the special case of water, i.e., when the solute and solvent molecules were identical, we have also calculated the excess free energy in another way, by performing a grand-canonical ensemble Monte Carlo (GCMC) simulation<sup>19</sup> as a further test. In a GCMC simulation the number of molecules  $N$  is allowed to fluctuate, and the excess free energy is computed as

$$A' = k_B T (B - \ln \langle N \rangle + 1) - pV/N \quad (6)$$

where the parameter  $B$  is kept fixed in the simulation. Here the  $B$  value was set (after some trial runs) to -6.15, resulting in 106.9 water molecules on average. In the simulation, every particle displacement step was followed by a particle insertion or deletion attempt. To improve the success of the insertions, the cavity biased technique<sup>20,21</sup> was employed, using a  $60 \times 60 \times 60$  grid and a 2.5 Å minimum cavity radius. After equilibration,  $2 \times 10^7$  configurations were generated for the calculation of the excess free energy.

**B. Lipid Simulation and Free Energy Profile Calculations.** The free energy profiles were calculated on snapshots extracted from a canonical ( $N, V, T$ ) ensemble Monte Carlo simulation of a bilayer containing 25-25 DMPC molecules surrounded by 2033 water molecules. The interaction parameters of the lipid and water molecules have been represented by the all-atom CHARMM22 force field<sup>24</sup> and the TIP3P model, respectively. The conformation of the lipid molecules has been sampled from their torsion angle space, while their bond lengths and bond angles have been kept fixed at their equilibrium values. The torsion angles and the lipid orientations were sampled with the novel extension biased method.<sup>28</sup> The simulation was performed at 310 K in a hexagonal prism-shape basic simulation cell under periodic boundary conditions. The edge length of the basic hexagon and the length of the prism have been obtained from a preliminary simulation at 1 bar in the ( $N, p, T$ ) ensemble as 23.60 and 79.75 Å, respectively. 1500 equilibrium configurations, separated by  $10^5$  Monte Carlo steps each, were saved for the evaluation of the free energy profiles. The lipid-lipid interactions have been treated by group-based minimum image convention, whereas group-based spherical cutoffs of 20 and

(28) Jedlovsky, P.; Mezei, M. *J. Chem. Phys.* **1999**, *111*, 10770.

**Table 2.** Excess Hydrational Free Energy of the Studied Molecules at 310 K Obtained with Different Methods of Investigation

	H <sub>2</sub> O	O <sub>2</sub>	CO	CO <sub>2</sub>	NO	CHCl <sub>3</sub>
GCMC	-5.75					
TI	-5.74	2.81	3.29	-0.03	2.29	1.31
Widom	-5.56	3.39	4.13	1.38	3.03	3.77
CIW $R_{\text{cav}} = 2.6 \text{ \AA}$	-5.39	3.27	3.94	1.03	2.88	3.64
CIW $R_{\text{cav}} = 2.8 \text{ \AA}$	-4.67	3.27	4.00	1.09	2.89	2.91

12  $\text{\AA}$  have been used for the lipid-water and water-water interactions, respectively. Further details of the lipid simulation are given elsewhere.<sup>28,29</sup> The calculations were performed by the program MMC.<sup>30</sup> The Helmholtz free energy profiles of H<sub>2</sub>O, O<sub>2</sub>, CO, CO<sub>2</sub>, NO, and CHCl<sub>3</sub> across the bilayer were calculated with the CIW method. Following eqs 2 and 3, the free energy profile was calculated as

$$A'(z) = -k_B T (\ln \langle \exp(-E_{N+1}(z)/k_B T) \rangle + \ln \langle P_{\text{cav}}(z) \rangle - 1) \quad (7)$$

where  $z$  is the system-fixed Cartesian axis perpendicular to the bilayer, with  $z = 0$  at the middle of the bilayer. (The  $z$ -independent  $-pV/N$  term was omitted here since at 1 bar it gives a negligibly small contribution to  $A'$ .) The system was divided into 25 slabs, containing 30 000 gridpoints each, along the  $z$  axis. The test molecule was inserted into those gridpoints which were located in cavities of radius of at least  $R_{\text{cav}}$ , where the  $R_{\text{cav}}$  value was set to 2.6  $\text{\AA}$  for H<sub>2</sub>O, 2.7  $\text{\AA}$  for O<sub>2</sub>, CO, CO<sub>2</sub>, and NO, and 2.8  $\text{\AA}$  for CHCl<sub>3</sub>. For each cavity found, 10 insertions were performed in different, randomly selected orientations of the test molecule. To investigate some specific features of the free energy profile of CO<sub>2</sub> and CHCl<sub>3</sub>, the CIW calculation of these two solutes were repeated with  $R_{\text{cav}} = 2.9 \text{ \AA}$ , 75 000 gridpoints per slabs and 20 insertions per cavities. The calculation of a free energy profile took about 10 days in a single R10000 processor, which is about a tenth of the computing time required to generate the 1500 equilibrium lipid configurations. This fact underlines one of the great advantages of the CIW method, namely, that once a sufficient trajectory is generated, the free energy profile calculation of several different molecules can be performed with a fairly small extra computational cost. Further significant speedup can be obtained if the free energy profiles of several molecules are calculated in a single run since in that case the cavity search has to be performed only once.

#### IV. Results and Discussion

**A. Test of the CIW Method in Aqueous Solutions.** The hydration free energies of the six solute molecules studied are summarized in Table 2 as obtained with different methods of investigation. It can be seen that generally the results of the original Widom and the CIW method are in good agreement with the thermodynamic integration (TI) data, with their difference usually between  $k_B T$  and  $2k_B T$ , i.e., on the order of the thermal motion of the molecules. It is also evident that with the exception of water the CIW results are in considerably better agreement with the TI values than that of the original Widom method, showing that the CIW method provided faster convergence (i.e., better statistics) than the original Widom method. This means that the use of cavity insertions in a Widom-type free energy calculation not only speeds up the calculation but can also provide more accurate results.

In the case of water the two reference methods, i.e., the GCMC simulation and the thermodynamic integration, resulted practically in the same excess free energy value. The results obtained both with the original Widom method and from the CIW calculation with a minimum cavity radius of  $R_{\text{cav}} = 2.6 \text{ \AA}$  are in excellent agreement with these data, and their deviations from the TI results, 0.176 and 0.350 kcal/mol, respectively, are

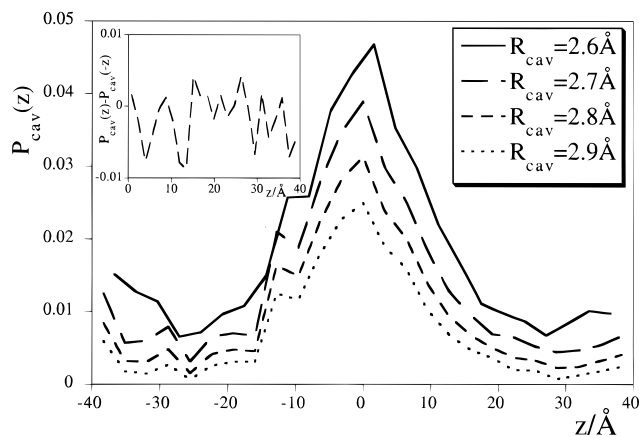


**Figure 1.** Probability profile of finding cavities with minimum radius of  $R_{\text{cav}}$  across the DMPC bilayer: solid line,  $R_{\text{cav}} = 2.6 \text{ \AA}$ ; long dashes,  $R_{\text{cav}} = 2.7 \text{ \AA}$ ; short dashes,  $R_{\text{cav}} = 2.8 \text{ \AA}$ ; dotted line,  $R_{\text{cav}} = 2.9 \text{ \AA}$ . The inset shows the  $[P_{\text{cav}}(z) - P_{\text{cav}}(-z)]$  difference function for  $R_{\text{cav}} = 2.7 \text{ \AA}$ .

well below  $k_B T$ . On the other hand, when the minimum cavity radius is set to 2.8  $\text{\AA}$ , the CIW method yields a too high hydration free energy value, which deviates from the GCMC and TI results by about 1 kcal/mol. The reason for this deviation probably originates from the fact that the excess water molecule does not fill completely a cavity of radius larger than 2.8  $\text{\AA}$ . The energy of the molecule inserted into such a cavity is then less negative than it could be in a slightly smaller cavity, which has a radius between 2.6 and 2.8  $\text{\AA}$ , and hence the deepest energy insertions are left out from the averaging in eq 3 when  $R_{\text{cav}} = 2.8 \text{ \AA}$  is used. In other words, these large cavities are not entirely mutated into a water molecule, and the free energy of such incomplete mutation is different from the  $-k_B T \ln \langle \exp(-E_{N+1}(z)/k_B T) \rangle$  factor present in eq 3.

The hydration free energy of the three diatomic molecules resulted in about 0.6–0.8 kcal/mol higher free energy by the original Widom method than the TI data. This deviation is about 22% and 20% smaller when the CIW method is used with  $R_{\text{cav}} = 2.6$  and 2.8  $\text{\AA}$ , respectively. A similar trend is observed for CO<sub>2</sub>; however, due to the larger size of the molecule, the deviation of the results of the various Widom insertion calculations from the TI data is considerably larger here than in the case of any of the diatomic solutes (see Table 2).

The situation is somewhat different in the case of CHCl<sub>3</sub>. Here the original Widom method resulted in a hydration free energy value about 2.5 kcal/mol higher than thermodynamic integration. The application of the cavity insertion technique did not improve the result considerably when  $R_{\text{cav}} = 2.6 \text{ \AA}$  was used. However, when the insertions were restricted to cavities of radius larger than 2.8  $\text{\AA}$ , the agreement improved by about 35% as the free energy value obtained here was only 1.6 kcal/mol higher than the TI result. The fact that, unlike for the other five molecules, here the CIW method with  $R_{\text{cav}} = 2.8 \text{ \AA}$  gave by far the best results is due to the fact that the chloroform molecule is considerably larger than any of the other five, and therefore low energy positions can only be found in large enough cavities.

The differences between the TI and CIW results provide an estimate of the uncertainty of the calculated free energy profiles of the above six molecules across a lipid bilayer. The good agreement obtained between the TI data and the CIW results with both  $R_{\text{cav}}$  values for the diatomic molecules and with  $R_{\text{cav}} = 2.6 \text{ \AA}$  for H<sub>2</sub>O, and also the reasonable agreement for CO<sub>2</sub>, can give us confidence in the precision of the corresponding

(29) URL: <http://inka.mssm.edu/~mezei/scri>.

(30) URL: <http://inka.mssm.edu/~mezei/mmc>.

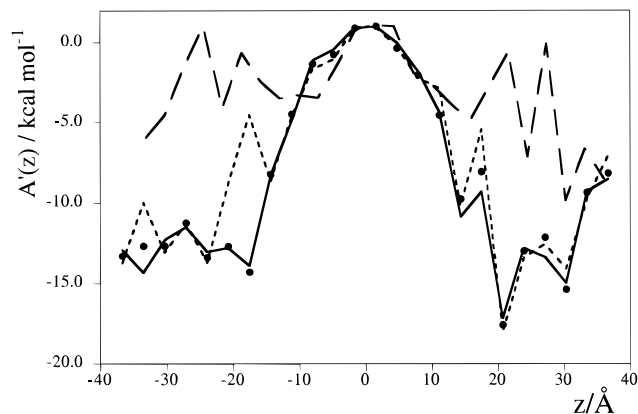


**Figure 2.** Free energy profile (solid line) of H<sub>2</sub>O across the DMPC bilayer resulting from our CIW calculation. Intermediate results after 20 million (long dashes), 40 million (short dashes), and 80 million (filled circles) MC steps are also shown.

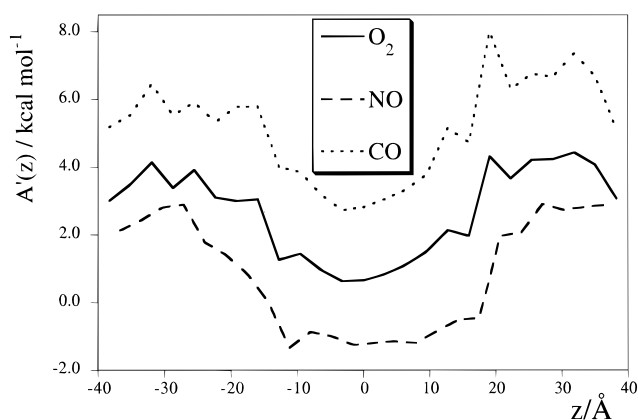


**Figure 3.** Free energy profile of O<sub>2</sub> (solid line), NO (dashed line), and CO (dotted line) across the DMPC bilayer resulting from our CIW calculation. The CO data are shifted by 2 kcal/mol for clarity.

free energy profiles. For CHCl<sub>3</sub> the deviation between the TI and CIW results is found to be about  $2.5k_B T$  even with  $R_{\text{cav}} = 2.8 \text{ \AA}$ , which, on the other hand, allows only a semiquantitative interpretation of the corresponding free energy profile.

**B. Free Energy Profiles across the DMPC Bilayer.** Figure 1 shows the  $P_{\text{cav}}$  profile across the DMPC bilayer as obtained from our calculations with four different  $R_{\text{cav}}$  values, i.e., 2.6, 2.7, 2.8, and 2.9 Å. The free energy profiles obtained are plotted in Figures 2–5, whereas the average excess free energies of the different solute molecules in the aqueous and hydrocarbon phase of the bilayer (defined here as beyond  $\pm 25 \text{ \AA}$  and between  $-8$  and  $+8 \text{ \AA}$ , respectively) are summarized in Table 3. As seen in Figure 1, all of the studied  $R_{\text{cav}}$  values gave  $P_{\text{cav}}(z)$  functions that are of similar shape. The cavity density is roughly constant beyond  $\pm 20 \text{ \AA}$ , i.e., in the aqueous region of the bilayer, whereas it increases steadily toward the middle of the bilayer in the interfacial region and in the hydrocarbon phase. Although the  $P_{\text{cav}}(z)$  curves are fairly symmetric to the middle of the bilayer, they show small differences between the two sides of the membrane (the  $[P_{\text{cav}}(z) - P_{\text{cav}}(-z)]$  difference function obtained with  $R_{\text{cav}} = 2.7 \text{ \AA}$  is shown in the inset of Figure 1). For instance, in the aqueous phase region the curves are somewhat noisier at negative  $z$  values than on the other side. Similarly, the small peak present at  $-15 \text{ \AA}$  is missing on the positive side and thus can be considered “noise”. However, despite these minor differences the overall agreement of the  $P_{\text{cav}}(z)$  function between the two sides of the bilayer indicates

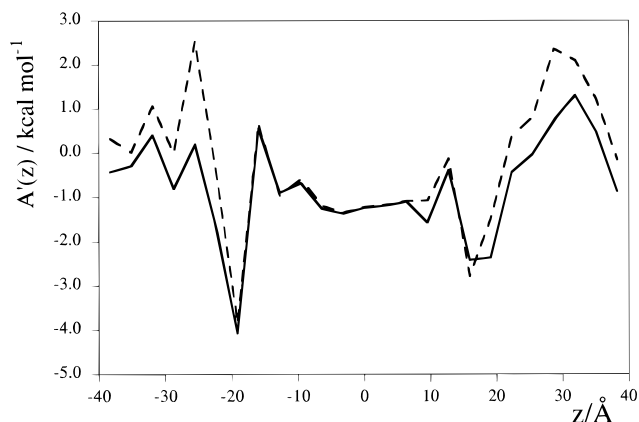


**Figure 4.** Free energy profile of CO<sub>2</sub> across the DMPC bilayer resulting from two different CIW calculations: solid line, using  $R_{\text{cav}} = 2.7 \text{ \AA}$ , 30 000 gridpoints per slabs, and 10 insertions per cavities; dashed line, using  $R_{\text{cav}} = 2.9 \text{ \AA}$ , 75 000 gridpoints per slabs, and 20 insertions per cavities.

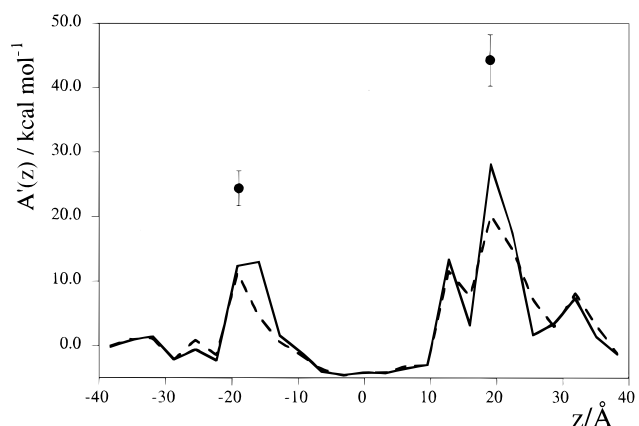


**Figure 5.** Free energy profile of CHCl<sub>3</sub> across the DMPC bilayer resulting from two different CIW calculations: solid line, using  $R_{\text{cav}} = 2.8 \text{ \AA}$ , 30 000 gridpoints per slabs, and 10 insertions per cavities; dashed line, using  $R_{\text{cav}} = 2.9 \text{ \AA}$ , 75 000 gridpoints per slabs, and 20 insertions per cavities. Filled circles with error bars show the results of thermodynamic integration.

**Table 3.** Excess Free Energy of the Studied Molecules in the Aqueous and Hydrocarbon Region (beyond  $\pm 25 \text{ \AA}$  and between  $-8$  and  $8 \text{ \AA}$ , Respectively) of the DMPC Bilayer at 310 K Obtained from Our CIW Calculations

	H <sub>2</sub> O	O <sub>2</sub>	CO	CO <sub>2</sub>	NO	CHCl <sub>3</sub>
aqueous phase	-13.95	3.74	3.95	-0.11	2.63	-1.07
hydrocarbon phase	-0.48	0.81	0.98	-1.23	-1.18	-4.21

that the equilibrium structure of the bilayer was sufficiently sampled in the simulation, allowing us to perform a meaningful analysis.

The obtained free energy profile of H<sub>2</sub>O is shown in Figure 2. To document the convergence of the calculation we also included the free energy profiles at three different stages of the calculation. It is seen that  $A'_{\text{H}_2\text{O}}$  is practically constant in the aqueous phase, beyond about  $\pm 18 \text{ \AA}$ , and changes also rather little in the hydrocarbon phase, between  $-8$  and  $+8 \text{ \AA}$ , whereas it increases rapidly toward the middle of the bilayer in the interfacial region. A water molecule has to go through a rather high free energy barrier when crossing the membrane: the difference of the average  $A'_{\text{H}_2\text{O}}$  values in the hydrocarbon and aqueous phases is about 13.5 kcal/mol (see Table 3). This result

is in excellent agreement with experimental data obtained for two biological membranes of 13.6 and 12.9 kcal/mol.<sup>31</sup>

It is also seen from Tables 2 and 3 that the excess free energy of water is significantly, by about 8.5 kcal/mol, lower in the aqueous region of the DMPC bilayer than in pure water. To show that this difference is not related to the different sizes of the two systems at all, we have repeated the GCMC simulation of pure water on a considerably larger system, with  $\langle N \rangle = 522$ , and obtained an  $A'$  value that is 0.6 kcal/mol *higher* than on the small reference system. Similar, but smaller difference has been found between the excess free energy of  $\text{CHCl}_3$  in pure water and in the aqueous phase of the membrane (about 4 kcal/mol), whereas the two values are equal within the accuracy of the CIW calculations for the other four molecules. These surprisingly large differences of the hydration free energy values of  $\text{H}_2\text{O}$  and  $\text{CHCl}_3$  are the consequence of the strong electric field of the zwitterionic phosphatidylcholine groups in the interfacial region of the bilayer, which perturbs the water structure far into the bulk region and thereby changes the excess free energy of the dipolar solutes considerably (the more dipolar the solute is the larger is this change: the dipole moment of the  $\text{H}_2\text{O}$  and  $\text{CHCl}_3$  models used are 2.35 and 1.07 D, respectively), and leaves  $A'$  unchanged for apolar solutes. This is also in agreement with our recent finding that the correlation between the dipolar orientation of the water molecules and the bilayer normal persists far beyond the distance where water reaches its bulk density.<sup>32</sup>

The free energy profiles of the three diatomic molecules (see Figure 3) are rather similar to each other. Similarly to water, the  $A'(z)$  curves of  $\text{O}_2$ ,  $\text{NO}$ , and  $\text{CO}$  are also almost constant both in the aqueous and in the hydrocarbon phases. However, contrary to the case of water, they decrease steadily toward the middle of the bilayer in the interfacial region. The depth of the free energy well in the bilayer is about 3 kcal/mol for  $\text{O}_2$  and  $\text{CO}$ , while it is somewhat larger, almost 4 kcal/mol for  $\text{NO}$  (see Table 3). This finding suggests that  $\text{O}_2$ ,  $\text{CO}$ , and  $\text{NO}$  can go much faster through a hydrated DMPC bilayer than  $\text{H}_2\text{O}$ . This relation is in agreement with their behavior in real biological membranes.

The  $A'(z)$  curve of  $\text{CO}_2$  (shown in Figure 4) is rather different from both that of water and the three diatomic molecules. The excess free energy is again practically constant across both the aqueous and the hydrocarbon phase with a small difference of about 1 kcal/mol between its value in these two phases (see Table 3). This is of the order of this CIW calculation's numerical uncertainty, as discussed in section IV.A. However, the  $A'(z)$  function drops sharply, by about 3–4 kcal/mol between  $\pm 20$  and  $15 \text{ \AA}$ , in the region of the zwitterionic headgroups. Thus, upon crossing the DMPC membrane a  $\text{CO}_2$  molecule has to go through two consecutive 3–4 kcal/mol high free energy barriers. This finding is unlikely to be the consequence of improper sampling of the test positions of the inserted  $\text{CO}_2$  molecule in this region since insufficient convergence of eqs 3 and 7 leads to too high, rather than too low free energy values (as lack of convergence means that positions of sufficiently low energies have not been found yet). To further demonstrate that the observed behavior of  $A'_{\text{CO}_2}(z)$  is indeed not simply an artifact, we have repeated this CIW calculation with use of many more gridpoints (i.e., 75000 instead of 30000 per slabs) in the cavity search, and also performing 20 instead of 10 random insertions into the cavities found. To reduce the large extra computation time required by these changes, we restricted insertions into

cavities of radius larger than  $2.9 \text{ \AA}$  only. In this way, the computational cost required by this new CIW calculation was about the same as in the case of the original one. The  $A'(z)$  curve obtained from this new CIW calculation, plotted also in Figure 4, is in excellent agreement with the result of the original calculation, confirming that the observed behavior of  $A'_{\text{CO}_2}(z)$  in the interfacial region is indeed real. It should be noted that  $\text{CO}_2$  can pass through biological membranes much faster than either  $\text{CO}$  or  $\text{O}_2$ .<sup>2</sup> This is in agreement with our finding that the free energy difference between the aqueous and hydrocarbon phases of the membrane is considerably smaller for  $\text{CO}_2$  than for the other two solutes. Although we have observed free energy barriers of about the same height for all three solutes across the DMPC bilayer, our results are not contradicted by the above fact. Namely, the aqueous and hydrocarbon phases of our membrane model are certainly rather similar to those of biological membranes, whereas the interfacial region can be very different from that, since biomembranes are mixtures of various lipid molecules differing mainly in the composition of their headgroups. Thus, the fact that the observed free energy difference between the aqueous and hydrocarbon phases of the membrane is considerably smaller for  $\text{CO}_2$  than for either  $\text{O}_2$  or  $\text{CO}$  means that if the membrane contains any kind of amphiphilic molecule which does not constitute extra free energy barrier or well for  $\text{CO}_2$  in the headgroup region (e.g., cholesterol),  $\text{CO}_2$  can indeed pass through the membrane along these molecules much faster than the other two solutes. Work in this direction is currently in progress.

The free energy profile obtained for  $\text{CHCl}_3$  is shown in Figure 5. As has been seen in section IV.A, due to the relatively large size of the  $\text{CHCl}_3$  molecule its excess free energy can only be determined with rather large uncertainty in water, and thus the  $A'_{\text{CHCl}_3}(z)$  curve obtained is also much less precise than the other five free energy profiles. However, some of the important features of the obtained curve can still be reliably interpreted. Since the CIW method reproduced the excess free energy of  $\text{CHCl}_3$  in water within 1.6 kcal/mol, it is a sensible limit of the uncertainty of the results obtained in the aqueous phase of the bilayer, as well. It is also quite probable that the free energy data obtained in the hydrocarbon phase are more accurate than those in the aqueous phase, since (i) there are considerably more cavities in the middle of the bilayer than in the aqueous region (see Figure 1), which allows a much better convergence of eq 7 here, and (ii) it is also sensible to assume that the local structure of the apolar hydrocarbon chains is much less distorted by the presence of a  $\text{CHCl}_3$  molecule than that of the strongly polar water molecules. On the other hand, no such assumption can be made for the interfacial region containing the zwitterionic headgroups. Therefore we can reliably conclude from the resulting  $A'_{\text{CHCl}_3}(z)$  function that the excess free energy of the  $\text{CHCl}_3$  molecule is a few kilocalories per mole lower in the middle of the bilayer than in the aqueous phase, but little can be said about the huge free energy barriers present in the two interfacial regions. To confirm that the existence of these barriers is a real feature, we have repeated the CIW calculation in the same way as for  $\text{CO}_2$ , i.e., with 75000 gridpoints per slab, 20 random insertions per cavities, and  $R_{\text{cav}} = 2.9 \text{ \AA}$ . The  $A'(z)$  curve obtained in this way, plotted also in Figure 5, shows good agreement with the results of the original CIW calculation. In accordance with our above assumptions, this agreement is excellent in the hydrocarbon phase, and also quite good in the aqueous region. The large free energy barriers at the interfacial region are also detected by the new CIW calculation.

To obtain further confirmation of the existence of this high

(31) Jansson, T.; Illsley, N. P. *J. Membr. Biol.* **1993**, *132*, 147.

(32) Jedlovsky, P.; Mezei, M. *J. Phys. Chem.* Submitted for publication.

free energy barrier in the interfacial region we also calculated (with polynomial TI) the excess free energy of inserting a  $\text{CHCl}_3$  molecule into the bilayer at  $z = \pm 19 \text{ \AA}$  at a randomly selected position in the  $x$ - $y$  plane. We obtained  $A'(-19) = 24.4 \pm 2.7$  kcal/mol and  $A'(19) = 44.3 \pm 4.0$  kcal/mol, respectively, providing additional confirmation of the existence of a large interfacial free energy barrier. The significant difference of these TI results from the CIW results at  $\pm 19 \text{ \AA}$  reflect the fact that the CIW data are an average over the whole cross section of the bilayer while the TI values only reflect the local conformation of the headgroups around the point selected in the  $x$ - $y$  plane. We should emphasize that the time required to calculate a single point with TI is of the same order as the time of calculating a complete free energy profile with the CIW method. Therefore, this finding also demonstrates the superiority of the particle insertion methodology in the free energy calculation for heterogeneous systems over other methods which otherwise work well for homogeneous systems.

The existence of such barriers is indeed in accordance with the anaesthetic properties of  $\text{CHCl}_3$ . This behavior is the consequence of  $\text{CHCl}_3$  being temporarily solvated in the interior of the cell membranes. The fact that  $\text{CHCl}_3$  leaves the cell membrane several orders of magnitude slower than  $\text{NO}$ ,  $\text{CO}$ , or  $\text{O}_2$  indicates that it has to go through a considerably higher free energy barrier upon leaving the membrane.

## V. Summary and Conclusions

In this paper we have calculated the free energy profile of six different small neutral molecules, i.e.,  $\text{H}_2\text{O}$ ,  $\text{O}_2$ ,  $\text{CO}$ ,  $\text{CO}_2$ ,  $\text{NO}$ , and  $\text{CHCl}_3$ , across a fully hydrated DMPC bilayer, and demonstrated that such free energy profiles can rapidly be computed in a relatively straightforward way by using the Cavity Insertion Widom method. The technique used by the CIW method is analogous with the cavity biased particle insertions used in grand-canonical and Gibbs ensemble Monte Carlo simulations, namely, the test particle is inserted into cavities of suitable radius only, and the bias introduced into the sampling by this modification is removed by an appropriate modification of the averaging. Suitable cavities are searched for with the use of an appropriate grid, and the ratio of the number of cavities found to the total number of gridpoints yields immediately the probability of finding a cavity  $P_{\text{cav}}$ , the only extra quantity needed for the removal of the bias.

The importance of this methodology lies in the fact that the local chemical potential is very sensitive to the lipid conformation, and thus the usual free energy methodologies would be extremely slow to converge since the slow rate of conformational change of the lipid molecules would present a serious bottleneck. However, the CIW method averages data over planes in the bilayer, and the averaging over lipids in different conformation avoids this problem. This unique averaging feature of the CIW method thus compensates for the lower numerical precision obtainable with it. An additional advantage of this

method is that the two most time-consuming parts of the calculation, the simulation of the lipid bilayer and the search for the suitable cavities, have to be done only once for the calculation of the free energy profiles of several different substances.

We have demonstrated by calculating the excess free energy of the above six solutes in pure water with various methods using cavity insertions the convergence of the Widom calculation can be speeded up considerably, and with a careful selection of the minimum cavity radius even the accuracy of the resulting free energy data can be improved. The comparison of the hydration free energies resulted from the various Widom-type calculations with the results of thermodynamic integration provided an estimate for the accuracy of the free energy data obtained for each of the six solutes in the lipid membrane. The resulting free energy profiles showed, in agreement with chemical common sense, that water prefers to stay in the aqueous phase whereas  $\text{O}_2$ ,  $\text{CO}$ ,  $\text{NO}$ , and  $\text{CHCl}_3$  prefer the hydrocarbon region of the bilayer. The free energy profiles of  $\text{H}_2\text{O}$ ,  $\text{O}_2$ ,  $\text{CO}$ , and  $\text{NO}$  change smoothly and monotonically in the interfacial region. On the other hand, we found that the excess free energy of  $\text{CO}_2$  is equal in the two phases within the precision of our calculation, but free energy wells appear clearly in the interfacial regions. Our results show that upon crossing the DMPC membrane a water molecule has to cross a free energy barrier of about 13 kcal/mol. This barrier is found to be only 3 kcal/mol for  $\text{O}_2$  and  $\text{CO}$  and 4 kcal/mol for  $\text{NO}$ , whereas  $\text{CO}_2$  molecules have to go through two consecutive free energy barriers of about 4 kcal/mol. The obtained free energy data are much less precise for  $\text{CHCl}_3$ ; however, we still can conclude that the excess free energy of  $\text{CHCl}_3$  is a few kilocalories per mole higher in the aqueous than in the hydrocarbon phase, whereas the interfacial regions constitute high free energy barriers for it.

Despite the large simplifications inherent in our models, the results obtained are in good agreement with the physiological behavior of the six molecules studied. In particular, the height of the free energy barrier found for  $\text{H}_2\text{O}$  is in good agreement with experimental data on different biological membranes.<sup>30</sup> Furthermore, in accordance with our results,  $\text{O}_2$ ,  $\text{CO}$ ,  $\text{CO}_2$ , and  $\text{NO}$  can cross the cell membranes promptly,<sup>2,4</sup> and  $\text{H}_2\text{O}$  can also cross cell membranes but much slower, thus the majority of the water transport of living cells is going through hydrophilic pores,<sup>2</sup> whereas  $\text{CHCl}_3$ , a formerly widely used anaesthetic, dissolves in the middle of the membrane and leaves it rather slowly, on the order of  $10^3$ - $10^4$  s.

**Acknowledgment.** P.J. is an Eötvös Fellow of the Hungarian Ministry of Education, which is gratefully acknowledged. The authors are grateful to Drs. Monika J. Fuxreiter and Tibor Rohács (Mount Sinai School of Medicine, New York) for stimulating discussions and critical reading of the manuscript.

JA000156Z